ELSEVIER

Int. J. Fatigue Vol. 20, No. 9, pp. 631–639, 1998

Printed in Great Britain
0142–1123/98/$—see front matter

PII: S0142-1123(98)00032-2

Continuum damage mechanics analysis of fatigue crack initiation

Baidurya Bhattacharya and Bruce Ellingwood

Department of Civil Engineering, The Johns Hopkins University, Baltimore, MD 21218, USA
(Received 15 June 1997; revised 22 February 1998; accepted 22 March 1998)

The crack initiation period in an originally defect-free component can be a significant portion of its total fatigue life. The initiation phase is generally believed to constitute the nucleation and growth of short cracks, but the threshold crack length at which initiation occurs lacks a uniform definition. Moreover, available methods for predicting fatigue damage growth usually require an existing flaw (e.g. Paris law) and may be difficult to apply to the initiation phase. This paper presents a continuum damage mechanics-based approach that estimates cumulative fatigue damage, and predicts crack initiation from fundamental principles of thermodynamics and mechanics. Assuming that fatigue damage prior to localization occurs close to a state of thermodynamic equilibrium, a differential equation of isotropic damage growth under uniaxial loading is derived that is amenable to closed-form solution. Damage, as a function of the number of cycles, is computed in a recursive manner using readily available material parameters. Even though most fatigue data are obtained under constant amplitude loading conditions, most engineering systems are subjected to variable amplitude loading, which can be accommodated easily by the recursive nature of the proposed method. The predictions are compared with available experimental results. © 1998 Elsevier Science Ltd. All rights reserved

(Keywords: continuum damage mechanics; cyclic loads; deformation; engineering mechanics; fatigue; steel; structural engineering; thermodynamics; variable amplitude loading)

INTRODUCTION

The total fatigue life, N_T, of an initially defect-free structure can be written as the sum,

$$N_T = N_I + N_P \tag{1}$$

where N_I is the crack initiation period, and N_P is the crack propagation period which includes the stable as well as the accelerated stages of fatigue crack growth. In many loading situations (for example, in high-cycle fatigue), the crack initiation period is the most important factor determining the total service life of a structure. The initiation phase of fatigue life in a virgin material is often assumed[1] to constitute the growth of short cracks up to the size a_{th}, which is the transition length of short cracks into long cracks.

The growth rate of long fatigue cracks (in the stable crack growth stage), along with the condition of their non-propagation, can be successfully modelled by the Paris–Erdogan law[2]. However, the preceding phase of fatigue, when initiation and growth of short cracks occur, is more difficult to model. Linear elastic fracture mechanics (LEFM)-based crack growth concepts break down at short crack sizes[3]. Short cracks grow at stress intensities below the long crack threshold stress intensity, ΔK_{th}. Moreover, depending on the stress ratio, $R = \sigma_{\min}/\sigma_{\max}$, short cracks may grow at rates higher than those for long cracks[4]. Ignoring the short crack growth stage, or using long crack growth rate parameters for short crack growth 'can lead to potential dangerous over-prediction of (fatigue) life'[5].

The threshold crack length, a_{th}, below which LEFM (and consequently the Paris–Erdogan law) is not valid, may be estimated approximately as[2]:

$$a_{th} = \frac{1}{\pi}\left(\frac{\Delta K_{th}}{2S_e}\right)^2 \tag{2}$$

where the endurance limit, S_e, and ΔK_{th} are both evaluated for fully reversed cycling (i.e. at $R = -1$). However, the threshold crack initiation length, a_{th}, lacks a universally accepted definition[6,7]. The comment of Kujawski and Ellyin[8] highlights this point: "Usually the crack initiation stage is associated with an arbitrary specified crack length. The crack length ranging from grain diameter to about 50–100 μm is used, depending on the material and physical scale of interest". However, a wider range of values have been selected for a_{th} in the literature, for example: 0.5 mm for structural welds[6]; 1 mm for En7A steel[5]; 120 μm for BS250A53 steel[1]; and 51 μm for carbon steel[9]. In fatigue inspection of structures, the crack detection threshold usually ranges between 1/8 and 1/4 in (~ 3–6 mm), and crack

Corresponding author. Tel: + 1 410 516 8680; Fax: + 1 410 516 7473

sizes in this range are also taken as the end of 'initiation' in many engineering analyses[10].

Empirical approaches are available for predicting crack initiation in a virgin material under fatigue loading, among them: (i) An *S–N* type approach, where the number of cycles correspond to the formation of an arbitrary threshold crack length under constant amplitude stress or strain cycling; and (ii) a Paris–Erdogan type of short crack growth law with different parameters than those used to predict growth of long cracks[1]. The first approach does not provide any measure of residual strength at various stages of damage accumulation prior to initiation. The second approach is extremely sensitive (as illustrated in Kaynak *et al*., 1996)[5] to the initial crack length that, like a_{th}, lacks a standard definition.

Although most fatigue data have been obtained under constant amplitude load cycling conditions, in most engineered systems applied stresses (or strains) seldom alternate between constant limits; instead the operating conditions lead to variable amplitude loading[10]. The problems in predicting cumulative fatigue damage under variable amplitude loading have long been recognized (e.g. Grover, 1954)[11]. A recent state-of-the-art review of the subject[12] makes it clear that there are considerable uncertainties associated with existing rules for predicting damage under variable amplitude loading.

Miner's rule[13] is often applied to assess cumulative fatigue damage under variable amplitude loading, due to its simplicity and its dependence only on readily available constant amplitude fatigue data. Making the assumption that damage, *D*, occurs in linear increments:

$$D = \sum_{i=1}^{N_B} \frac{n_i(S_i)}{N_i(S_i)} \tag{3}$$

$$= 1 \text{ at failure} \tag{4}$$

Here n_i and N_i denote, respectively, the number of applied cycles at stress level S_i, and the number of cycles to initiation or failure at constant amplitude stress level, S_i (utilizing the experimentally determined *S–N* curve for the structural detail of interest). N_B denotes the number of different stress levels applied. The linear damage increment rule has been called into question by numerous experimental observations[12,14,15]. It has been found, for example, that the major portion of service-life may be spent without any manifestation of reduced capacity so that damage becomes apparent and grows visibly at an accelerating rate only towards the end of the life-time[16–18]. Moreover, Miner's rule does not account for load sequencing effects on fatigue, where it has been observed that a few cycles (n_2) at a high stress level (S_2) followed by cycling at a lower level (S_1, n_1) causes greater damage than when the order is reversed (*Figure 1*). Several improvements in Miner's linear damage rule have been suggested[14,19–21], which have met with varying degrees of success for specific applications.

The continuum damage mechanics (CDM)-based analysis of fatigue crack initiation developed in this paper is independent of threshold crack sizes and empirical growth parameters for microscopic cracks. It can provide estimates of N_I in terms of macroscopically obtained material parameters, and can accommodate variable amplitude fatigue loading in a natural and non-empirical way.

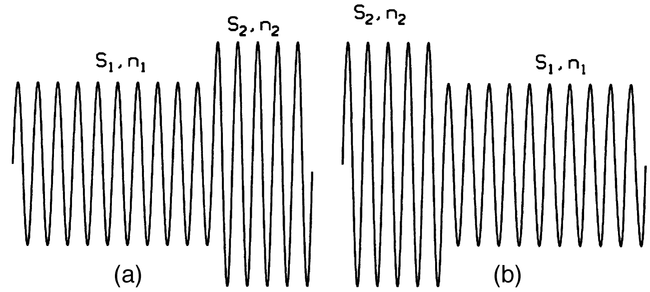

Figure 1 Two-level fatigue load cycling, $S_2 > S_1$

CRACK INITIATION AND CDM

Continuum damage mechanics (CDM), a relatively new development in solid mechanics, deals with the distribution, characterization and growth of microstructural defects in terms of macroscopic state variables[22–24]. Physically, the CDM damage concept represents a loss of material integrity which reduces the capacity of a damaged component to bear applied stresses. In CDM, the damage variable, $D(\hat{n})$, on an elemental cross-sectional plane (with unit normal ($\hat{n}$)) is quantified by the surface density of cracks and voids, weighted by the effects of stress concentration at the edges of discontinuities and the interaction among the defects. In general, $D(\hat{n})$ is a tensor; however, if the weighted fractional loss in cross-sectional area is the same in every orientation within the material, then damage is independent of ($\hat{n}$) and is said to be isotropic. Isotropic damage is quantified by the scalar variable, *D*, assuming values between zero and one. Damage is considered to be isotropic in this paper.

The accumulation of damage, so defined, is a dissipative (i.e. irreversible) process that obeys the laws of thermodynamics[25]. The overall damage variable is a non-decreasing function of time in the absence of corrective human intervention. Failure occurs when *D* reaches the critical damage $D_c \leq 1$. In the context of CDM, 'failure' is not necessarily fracture, but is the condition when one assumption essential to continuum damage mechanics—that damage arises out of a volume-wide degradation of the material microstructure—loses its validity. Chaboche (1988)[26] described this condition as the 'breaking up of the continuum volume element'. At this point, the damage-causing process becomes localized and leads to the growth of a dominant defect, which, in the context of fatigue loading, signals the initiation of a crack in an originally defect-free component[17,27–29]. Thus, CDM is able to model damage growth in the initial 'defect-free' stage, unlike methods that need a measurable flaw to be useful. The CDM-based interpretations of failure allow D_c to have values less than unity, as opposed to state variable-type phenomenological models (including Miner's rule) that, in effect, require $D_c = 1$ for failure to occur. A postulate of CDM[29] is that D_c is an intrinsic material property, and that its value determined from a simple experiment (e.g. a static tension test) for a given material and temperature can be used to predict failure (i.e. crack initiation) in a more complex situation such as fatigue loading. Experimentally determined values of D_c range between 0.15 and 0.85 depending on the material[30].

The stress distribution within a damaged material is related to the state of damage within the material[26,31] through the concept of effective stress, defined as

$$\tilde{\sigma} = \frac{\sigma}{1 - D} \quad (5)$$

where σ is the nominal stress. With the assumption that the principle of strain equivalence[26] can describe satisfactorily the constitutive law for the damaged material of interest (as it indeed has for many engineering alloys)[30], the elastic modulus of the damaged component can be described as a linear function of the damage variable[27]:

$$\tilde{E} = E(1 - D) \quad (6)$$

where E is the original (undamaged) modulus of elasticity of the component, and the Poisson's ratio is assumed to be unaffected by damage[32]. An appropriate gauge length including the damaged zone in the component may be necessary to measure the change in stiffness accurately, and hence the CDM-based damage variable. Equation (6) provides a means to monitor the state of damage in a component in service by measuring its change of stiffness. In the context of fatigue loading, this measurement can be used for early detection/prediction of crack initiation in a structure.

THERMODYNAMIC MODELLING OF DAMAGE ACCUMULATION

Assume that damage growth is occurring prior to localization in a deformable body $\Re$ (having the closed boundary $\partial\Re$) which is in diathermal contact with a heat reservoir at constant absolute temperature θ. Let W be the work done on $\Re$, and U, K_E and S be the internal energy, kinetic energy and entropy of $\Re$, respectively.

The Helmholtz free energy function of $\Re$, given by $\Psi = U - \theta S$, determines the maximum work that can be obtained in a given isothermal process[33]. It is a function of the absolute temperature, the damage variable, and the symmetric strain tensor, ϵ_{ij}. The Helmholtz free energy is stationary for a system undergoing a reversible process in diathermal contact with a heat reservoir[34]. The first variation in the free energy of $\Re$ at an arbitrary instant t_2 is given by

$$\delta\Psi(t_2) = \delta\Psi(t_1) + \delta\int_{t_1}^{t_2}(\dot{W} - \dot{K}_E)dt - \delta\int_{t_1}^{t_2}\Gamma dt \quad (7)$$

where Γ is the rate of energy dissipation, which may be expressed, with the help of the first and second laws of thermodynamics and with $\dot{\theta} = 0$, as[35]:

$$\Gamma \equiv -\dot{K}_E + \dot{W} - \frac{\partial\Psi}{\partial\epsilon_{ij}}\cdot\dot{\epsilon}_{ij} - \frac{\partial\Psi}{\partial D}\cdot\dot{D} \geq 0 \quad (8)$$

Assuming the initial condition (at time t_1) is one of thermodynamic equilibrium (i.e. $\delta\Psi(t_1) = 0$), the variation given by Equation (7) can be expressed as:

$$\delta\Psi(t_2) = \int_{t_1}^{t_2}\delta I_1(t)dt - \int_{t_1}^{t_2}\delta I_2(t)dt \quad (9)$$

where the commutability of integration and variation has been used, and

$$I_1 = \dot{W} - \dot{K}_E + \frac{\partial\Psi}{\partial D}\dot{D} \quad (10)$$

$$I_2 = \dot{W} - \dot{K}_E - \frac{\partial\Psi}{\partial\epsilon_{ij}}\dot{\epsilon}_{ij} \quad (11)$$

The term

$$\delta\Psi(t_2) = g(\theta,\epsilon_{ij},D,\delta\dot{\theta},\delta\dot{\epsilon}_{ij},\delta\dot{D};t) \simeq 0 \quad t \in [t_1,t_2] \quad (12)$$

depends on the state of the system as well as on the choice of the variations in temperature, strain rate and damage, and is generally non-zero for an irreversible process or for a system yet to achieve equilibrium. However, we assume that damage growth prior to localization of defects occurs slowly and close to equilibrium; thus the function $g(\cdot)$ is assumed to vanish for a suitable set of variations. Under this assumption, which has been validated for load-induced ductile damage[35], it can be shown that,

$$\delta I_2 = \int_{\Re}(F_i + \sigma_{ij,j} - \rho a_i)\delta\dot{u}_i dV + \int_{\partial\Re_1}(T_i - \sigma_{ij}n_j)\delta\dot{u}_i d\eta \quad (13)$$

where $\partial\Re_1 \subset \partial\Re$ is the free surface, and n_j (j = 1,2,3) is the unit normal out of $\partial\Re$. The quantities $\dot{u}_i$ and a_i denote, respectively, the velocity and acceleration at a point; ρ is the density; $F_i(t)$ and $T_i(t)$ are, respectively, the body forces in $\Re$ and the surface traction on $\partial\Re_1$. The stress tensor $\sigma_{ij} = \partial\psi/\partial\epsilon_{ij}$[36], where ψ is the free energy per unit volume.

The right hand side of Equation (13) is zero as the terms in parentheses constitute the equilibrium equations of a deformable body (damaged or otherwise) on $\Re$ and $\partial\Re_1$, respectively[37]. Therefore the first term in Equation (9) must also vanish.

Assuming that $\delta I_1(t)$ vanishes at all t, we apply small variations in the velocity field (consistent with the boundary conditions) that do not alter the instantaneous force, acceleration and strain distributions of the body, and do not affect the rate of change in the free energy with respect to damage, $\psi_D = \partial\psi/\partial D$, at that instant. Noting that $\delta\dot{D} = d(\delta D)/dt$ and $\delta D = (\partial D/\partial\epsilon_{ij})\delta\epsilon_{ij}$, we arrive at the set of coupled partial differential equations,

$$T_i + \psi_D\frac{\partial D}{\partial\epsilon_{ij}}n_j = 0 \text{ on } \partial\Re_1 \quad (14)$$

The solution to Equation (14) if the body is subjected to multiaxial straining is feasible but generally computationally difficult. However, the uniaxial form of Equation (14),

$$\frac{dD}{d\epsilon} = -\frac{\sigma_\infty}{\psi_D} \quad (15)$$

in which σ_∞ is the far-field stress acting normal to the surface, is amenable to close-formed solutions as shown subsequently. The solution to uniaxial loading is of particular interest here because experimental fatigue data available to validate the analysis have been obtained mainly for uniaxial loading.

ISOTROPIC FATIGUE DAMAGE GROWTH UNDER UNIAXIAL LOADING

The growth of fatigue damage is intimately connected to load cycling. With each cycle, additional damage is introduced in the material, provided the cyclic stress range (in that cycle) exceeds the endurance limit, S_e. The damage at the end of cycle i acts as the initial damage for the increment in cycle $i + 1$:

$$D_{i+1} = D_i + \Delta D_i,\ \Delta D_i \geq 0,\ i = 1,\ldots,N_I - 1 \tag{16}$$

Note that the similarities of Equation (16) to Miner's rule are more apparent than real, since in the CDM formulation ΔD_i need not be equal during each cycle under equal stresses (or strains). Crack initiation occurs when the critical value for damage is reached:

$$\begin{aligned} D_{N_I - 1} &< D_c \\ D_{N_I} &\geq D_c \end{aligned} \tag{17}$$

It is assumed that the unloading portion of a hysteresis loop and compressive stresses do not to contribute to damage growth (*Figure 2*), and that damage grows only during the reloading section above the endurance limit in the positive stress region (similar assumptions regarding fatigue damage increment are also found in Kachanov, 1986[31] and Lemaitre, 1984)[27]. The equation of fatigue damage growth in cycle i can therefore be written as (cf. Equation (15)):

$$\frac{dD}{d\epsilon} = \begin{cases} -\sigma_\infty/\psi_D & ;\ \sigma_\infty \geq S_e \geq 0,\ \dot{\epsilon} > 0 \\ 0 & ;\quad \text{otherwise} \end{cases} \tag{18}$$

with the initial damage $D = D_{i-1}$. The free energy per unit volume in cycle i is,

$$\psi = \int_{\epsilon_{0_i}}^{\epsilon} \sigma d\epsilon' - (\gamma - \gamma_{i-1}) \tag{19}$$

where γ is the surface energy of formation of defects within the material, and ϵ_{0_i} is the threshold strain of damage increment in cycle i[27], which depends on the accumulated damage and the endurance limit. An estimate of γ can be obtained by assuming that defects within the damaged material are spherical voids (of different sizes) distributed uniformly in space within the material volume, that the force–displacement relation at the microscale is linear, and that a void is formed when the stress on its impending boundary equals the true failure stress σ_f. It can then be shown that[35]:

$$\gamma = \frac{3}{4}\sigma_f D \tag{20}$$

Equation (20) is a simple way of estimating the surface energy of formation of voids in terms of readily obtained quantities, and is suitable for use until more accurate information regarding the number, shapes, sizes and interaction of the voids as a function of time becomes available.

The integral expression in Equation (19) is computed using a Ramberg–Osgood type equation for the hysteresis loop in cycle i:

$$\Delta\epsilon_i = \frac{\Delta\tilde{\sigma}_i}{E_i} + 2\left(\frac{\Delta\tilde{\sigma}_i}{2H_i}\right)^{M_i'} \tag{21}$$

The first term in Equation (21) represents the elastic strain range, $\Delta\epsilon_{e_i}$, while the second term represents the plastic strain range, $\Delta\epsilon_{p_i}$, and their sum is the cyclic strain range, $\Delta\epsilon_i$. The quantity $\Delta\tilde{\sigma}_i$ is the effective stress range, E_i is the elastic modulus, and H_i, M_i' are the cyclic hardening modulus and the cyclic hardening exponent respectively. The subscript i emphasizes the fact that these quantities, along with the lower and upper loop-tip coordinates, $\epsilon_{\min}$, $\sigma_{\min}$ and $\epsilon_{\max}$, $\sigma_{\max}$ (illustrated in *Figure 2*), may vary from cycle to cycle, depending on cyclic softening or hardening of the material and loading conditions. Since the damage equations are applied incrementally, the changes in stress–strain behavior as the material cyclically softens or hardens can be taken into account (by using cycle-dependent values for E_i, H_i, M_i'); however, for simplicity, we assume that it is sufficient to use the values (E, H, M') from a stabilized cyclic stress–strain curve.

The value of $(\epsilon_{\min}, \sigma_{\min})$, of course, is constant within any given cycle, and consequently, we can write, $d\epsilon = d\Delta\epsilon$ and $dD/d\epsilon = dD/d\Delta\epsilon$ for that cycle. Using the principle of strain equivalence and assuming $dD/d\Delta\epsilon \simeq dD/d\Delta\epsilon_p$, the differential equation of damage growth in cycle i, provided $\sigma_{\max_i} \geq S_e$, is[35],

$$\frac{dD}{1-D} = \frac{\{K'(\Delta\epsilon_p)^{1/M'} - K'(\Delta\epsilon_{p1_i})^{1/M'}\}d\Delta\epsilon_p}{\left[\begin{aligned}&\frac{K'^2}{2E}\{\Delta\epsilon_p^{2/M'} - \Delta\epsilon_{0_i}^{2/M'}\} + \frac{K'}{1+1/M'}\{\Delta\epsilon_p^{1+1/M'} - \epsilon_{p0_i}^{1+1/M'}\} \\ &- \frac{K'^2}{E}\Delta\epsilon_{p1_i}^{1/M'}(\Delta\epsilon_p^{1/M'} - \Delta\epsilon_{0_i}^{1/M'}) \\ &- K'\Delta\epsilon_{p1_i}^{1/M'}(\Delta\epsilon_p - \Delta\epsilon_{0_i}) + \tfrac{3}{4}\sigma_f\end{aligned}\right]} \tag{22}$$

with the initial condition $D = D_{i-1}$ at $\Delta\epsilon_p = \Delta\epsilon_{0_i}$. The parameter, $K' = 2^{1-1/M'}H$. The damage at the end of cycle i, D_i, is the solution of Equation (22) at

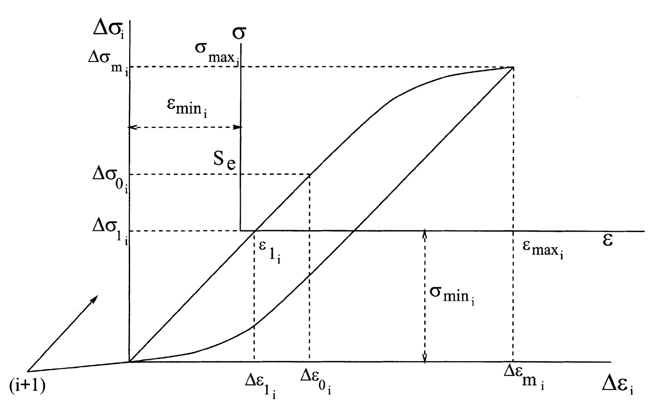

Figure 2 Stress–strain coordinates in one load cycle

$\Delta\epsilon_p = \Delta\epsilon_{pm_i}$, which is the maximum plastic strain range for that cycle (*Figure 2*). Assuming $K'/E \sim 0$ (i.e. $H/E \sim 0$, which is valid for most engineering materials), the closed-form solution is:

$$D_i = \begin{cases} 1-(1-D_{i-1})\dfrac{\dfrac{1}{1+1/M'}\Delta\epsilon_{0_i}^{1+1/M'}-\Delta\epsilon_{p1_i}^{1/M'}\Delta\epsilon_{0_i}+C_i}{\dfrac{1}{1+1/M'}\Delta\epsilon_{pm_i}^{1+1/M'}-\Delta\epsilon_{p1_i}^{1/M'}\Delta\epsilon_{pm_i}+C_i} & ;\sigma_{\max_i} \geq S_e \\ D_{i-1} & ;\text{otherwise} \end{cases} \tag{23}$$

where,

$$C_i = \frac{3}{4}\frac{\sigma_f}{K'} - \frac{\Delta\epsilon_{p0_i}^{1+1/M'}}{1+1/M'} + \Delta\epsilon_{p1_i}^{1/M'}\Delta\epsilon_{p0_i} \tag{24}$$

The proposed model of fatigue damage growth in Equation (23) computes fatigue damage in a recursive manner. The damage after n cycles is computed as

$$D_n = 1 - (1 - D_0)\prod_{i=1}^{n} f(\underline{\epsilon}_i;\Omega) \tag{25}$$

where $\underline{\epsilon}_i$ represents the strain limits in cycle i, $\Omega = \{E,H,M',S_e,\sigma_f\}$ is the set of material parameters, and D_0 is the initial damage existing at the onset of fatigue cycling. For a virgin material, $D_0 = 0$. The cycle-dependent function, $f(\underline{\epsilon}^i;\Omega)$, is

$$f(\underline{\epsilon}_i;\Omega) = \begin{cases} \dfrac{\dfrac{1}{1+1/M'}\Delta\epsilon_{0_i}^{1+1/M'}-\Delta\epsilon_{p1_i}^{1/M'}\Delta\epsilon_{0_i}+C_i}{\dfrac{1}{1+1/M'}\Delta\epsilon_{pm_i}^{1+1/M'}-\Delta\epsilon_{p1_i}^{1/M'}\Delta\epsilon_{pm_i}+C_i} & ;\sigma_{\max_i}>S_e \\ 1 & ;\text{otherwise} \end{cases} \tag{26}$$

FATIGUE DAMAGE GROWTH UNDER CONSTANT AMPLITUDE LOADING

Table 1 presents tensile and cyclic stress–strain properties for four engineering materials used in subsequent comparisons of predicted and observed fatigue behavior. The first three materials are used in constant amplitude load cycling examples in this section; the SAE 4130 steel is used in a later load-sequencing example.

Figure 3 presents results from constant-amplitude fully reversed strain-controlled fatigue cycling of SAE 4340 aircraft quality quenched and tempered steel. This material softens under constant-amplitude strain-controlled cycling. The theoretical threshold crack length is $a_{th} = 27$ μm (Equation (2), with $\Delta K_{th} = 10$ MPa$\sqrt{\text{m}}$)[2]. The predicted N_I is obtained with the help of Equation (25) and material properties from *Table 1*, using the initiation condition described by Equation (17). Since an experimental value of critical damage of SAE 4340 steel was not available, two different values, 0.15 and 0.46, are used in Equation (17). The former, $D_c = 0.15$, is the same as that observed at fatigue crack initiation in AISI 1010 carbon steel and AISI 316 stainless steel[30]. The latter, $D_c = 0.46$, was obtained analytically from a CDM model of monotonic ductile damage growth that used standard tensile properties of SAE 4340 steel, as described by Bhattacharya (1997)[35]. The prediction of crack initiation, as illustrated in *Figure 3*, is not especially sensitive to D_c. The predicted N_I corresponding to $D_c = 0.46$ compares very well with the number of cycles to the initiation of a 38 μm crack in the same nominal grade of material but with different material properties, e.g. $\sigma_y = 650$ MPa[2]. The number of cycles required for the growth of the above cracks to (i) 125 μm and (ii) to failure are also plotted. *Figure 3* also compares the proposed model with the empirical Coffin–Manson law, which predicts fatigue life under constant-amplitude strain-controlled cycling:

$$\frac{\Delta\epsilon}{2} = \frac{\sigma_f'}{E}(2N)^b + \epsilon_f'(2N)^c \tag{27}$$

in which the empirical constants are: $\sigma_f' = 1758$ MPa, $\epsilon_f' = 2.12$, $b = -0.0977$ and $c = -0.774$[2]. Equation (27) separates the total strain ampli-

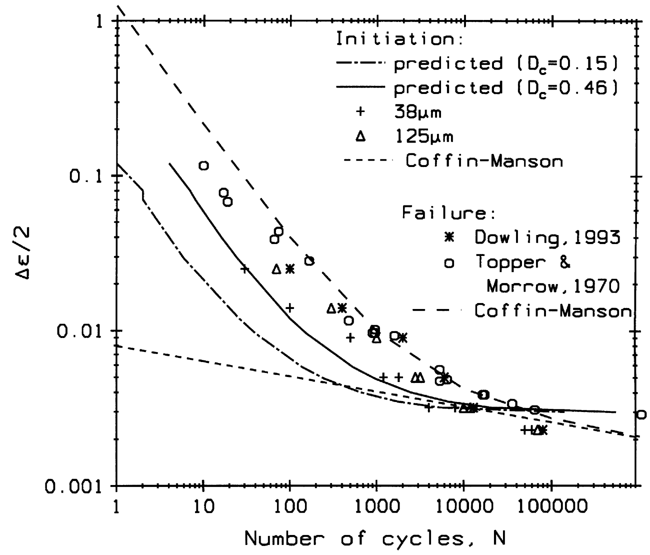

Figure 3 Fatigue crack initiation and failure under constant amplitude strain-controlled load cycling of SAE 4340 steel

Table 1 Tensile and cyclic material properties

Material	Source	E GPa	H MPa	M'	σ_f MPa	S_e MPa	σ_y MPa
SAE 4340 steel	38	192.9	1812	7.1	1911	542	1180
A106 Gr-B steel (288°C in air)	39	196.5	1994	7.74	539	310	301
2024-T4 Al	38	70.4	856	9.1	683	138	304
SAE 4130 steel	40	221	1366	7.25	1692	530	780

tude, $\Delta\epsilon/2$, into its elastic ($\Delta\epsilon_e/2$) and plastic ($\Delta\epsilon_p/2$) components, so that the first term in Equation (27) can be said to model the crack initiation stage, and the second term the crack propagation stage[2]. The total fatigue life predicted by the Coffin–Manson law agrees well with the results of Topper and Morrow[41]. However, the Coffin–Manson prediction of crack initiation is not satisfactory, particularly in the low-cycle region, whereas the CDM-based Equation (25) predicts the Dowling crack initiation data more accurately.

Figure 4 describes fully reversed strain-controlled fatigue cycling of A106 grade B steel (a steel commonly used in nuclear power plant piping) at 288°C in air. The predicted N_I is obtained from Equation (25) (using material properties from *Table 1*) and Equation (17) (assuming $D_c = 0.25$). The predicted N_I agrees well with the number of cycles to initiate a 0.18 mm crack[9]. *Figure 4* also plots the predicted $N_T = N_I + N_P$, in which N_P is obtained by integrating the Paris law (with parameters $C = 6.9 \times 10^{-9}$ mm/cycle, m = 3.0) between the limits a_{th} (Equation (2) with ΔK_{th}=6.0 MPa$\sqrt{\text{m}}$) and a_f = 6.35 mm, subject to the condition $K_{\max} \leq \min(K_c, \sqrt{E\sigma_y\delta_T})$, where K_c = 66 MPa$\sqrt{\text{m}}$ and δ_T = 0.04 mm[2,42]. The predicted N_T is compared with the experimental N_T from Majumdar et al. (1993)[9] and N_{25} (the number of cycles to a 25% drop in the peak tensile stress, a point at which failure is imminent) from Chopra et al. (1995)[39] and Chopra (1996)[43], and is found to lie within the experimental scatter. The CDM-based approach can therefore act as a complement to fracture mechanics in providing a complete description of fatigue damage growth.

The rate of fatigue damage growth under constant amplitude stress-controlled cycling is generally different from that under strain-controlled cycling. This difference can be illustrated by the formulation presented in this paper. In strain-controlled cycling, since the strain range, $\Delta\epsilon_m = \epsilon_{\max} - \epsilon_{\min}$, remains constant, the maximum plastic strain range in cycle i, $\Delta\epsilon_{pm_i}$, is obtained in terms of $\Delta\epsilon_m$ by (numerically) solving the following equation (cf. Equation (21)):

$$\Delta\epsilon_{pm_i} + \frac{K'}{E}\,\Delta\epsilon_{pm_i}^{1/M'} - \Delta\epsilon_m = 0 \tag{28}$$

On the other hand, in purely stress-controlled cycling, the maximum nominal stress range, $\Delta\sigma_m = \sigma_{\max} - \sigma_{\min}$ remains constant, and $\Delta\epsilon_{pm_i}$ is obtained in terms of $\Delta\sigma_m$ as,

$$\Delta\epsilon_{pm_i} = \left(\frac{\Delta\sigma_m}{K'(1 - D_{i-1})}\right)^{M'} \tag{29}$$

The solutions of Equations (28) and (29) are generally different. The other plastic strain ranges used in Equations (23) and (24), namely,

$$\Delta\epsilon_{p1_i} = \left(\frac{\Delta\sigma_{1i}}{K'(1 - D_{i-1})}\right)^{M'} \tag{30}$$

and

$$\Delta\epsilon_{0_i} = \left(\frac{\Delta\sigma_{1i}}{K'(1 - D_{i-1})} + \frac{S_e}{K'}\right)^{M'} \tag{31}$$

can also be shown to be different under strain-controlled and stress-controlled load cyclings. Thus, even with the same prior damage, D_{i-1}, the same nominal material properties Ω, and an equivalence between $\Delta\sigma$ and $\Delta\epsilon$ in a given cycle (through Equation (21)), the damage increments in the two situations are different. *Figure 5* shows the predicted damage growth over 20 cycles of fully reversed strain-controlled cycling (without pre-straining) of SAE 4340 steel at an amplitude of ± 0.005. The softening material stabilizes at a stress amplitude of ± 827 MPa (± 120 ksi)[41] at $\Delta\epsilon/2$ = 0.005. If the cycling were conducted instead under stress control at ± 120 ksi, the predicted damage would be about seven times larger after 20 cycles. *Figure 5* also shows that increasing the stress ratio, R, while keeping the stress amplitude constant at 120 ksi causes the rate of damage accumulation under stress-controlled cycling to increase significantly.

Figure 6 describes fatigue crack initiation and failure of 2024-T4 aluminum under constant amplitude stress-controlled cycling. As before, the predicted N_I is obtained using Equations (17) and (25) and material properties from *Table 1*. The critical damage is unknown, and two different values of D_c are used: (i) 0.10 based on experimental observations on other engineering alloys[30]; and (ii) 0.32, obtained from a

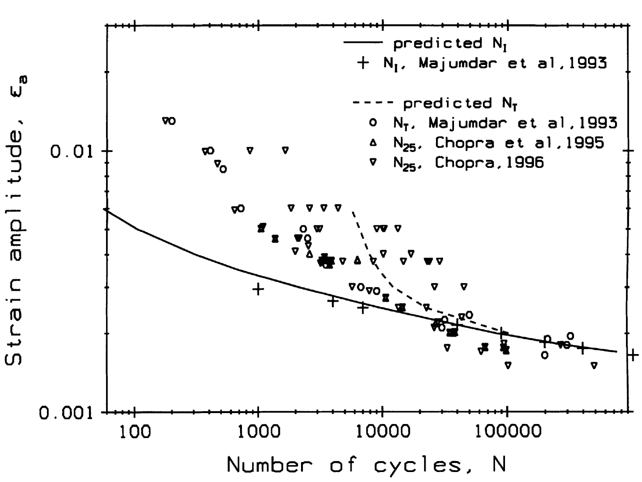

Figure 4 Fatigue crack initiation and failure under constant amplitude strain-controlled load cycling of A106 Gr B steel

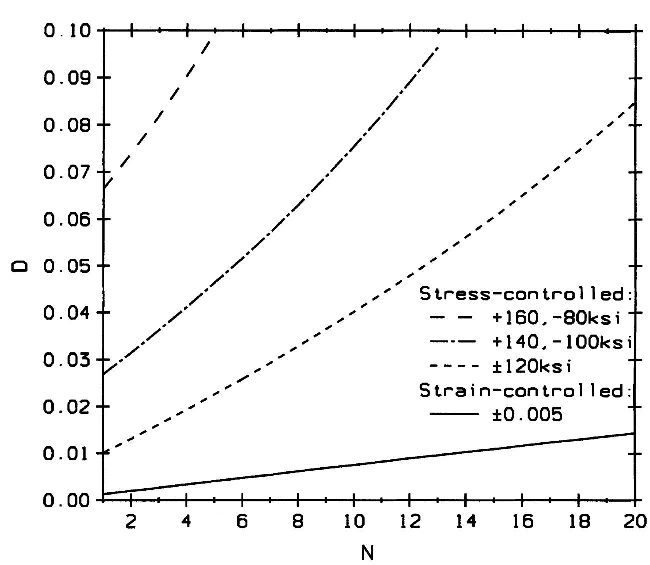

Figure 5 Predicted mean stress effects, and difference between strain-controlled and stress-controlled cyclings

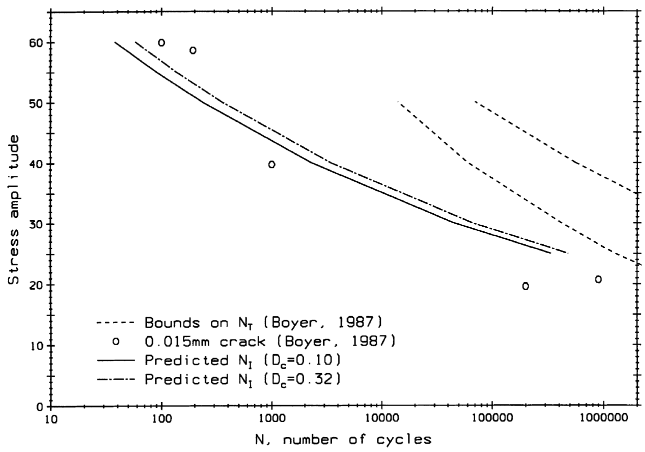

Figure 6 Fatigue crack initiation and failure under constant amplitude. stress-controlled load cycling of 2024-T4 Al

monotonic ductile damage growth model[35] that used standard tensile properties of 2024-T4 Al. As with the SAE 4340 steel considered, the predicted crack initiation is rather insensitive to the choice of D_c, and agrees well the cycles to initiate a 15 μm crack[44], which is of the same order as the grain size (20 μm).

The capacity of a degraded structure can be related explicitly to the CDM damage variable by Equation (6). Thus, the residual strength of a fatigued component (in the pre-crack initiation stage) can be predicted as a function of elapsed cycles if D_n is known (cf. *Figure 5*). The decrease in strength clearly is non-linear with respect to the elapsed number of cycles.

FATIGUE DAMAGE GROWTH UNDER VARIABLE LOADING

Equations (25) and (26) can easily incorporate variable amplitude stress (or strain) cycling, and predict the number of cycles to a macro-crack initiation in conjunction with Equation (17). The present research was, however, unable to locate any published data that indicated how the crack initiation life was affected by load sequencing effects, though a sizeable set of results are available for total fatigue life when the propagation phase is included[15,19,20], To investigate the role of load sequencing effects on crack initiation, let us consider the variable load occurring at just two levels: S_1 for n_1 cycles and S_2 for n_2 cycles (cf. *Figure 1*). The load level S_1 represents two fixed limits of applied stress (or strain) cycling as does S_2. When S_1 is applied first for n_1 cycles, the damage is

$$D_{n_1} = 1 - (1 - D_0) \prod_{i=1}^{n_1} f(\underline{\epsilon}_{1_i};\Omega) \tag{32}$$

D_{n_1} acts as the initial damage when S_2 is applied for a further n_2 cycles; the total damage at the end of $n_1 + n_2$ cycles is

$$D_{n_1,n_2} = 1 - (1 - D_{n_1}) \prod_{i=n_1+1}^{n_1+n_2} f(\underline{\epsilon}_{2_i};\Omega) \tag{33}$$

$$= 1 - (1 - D_0) \prod_{i=1}^{n_1} f(\underline{\epsilon}_{1_i};\Omega) \prod_{i=n_1+1}^{n_1+n_2} f(\underline{\epsilon}_{2_i};\Omega) \tag{34}$$

Conversely, if S_2 is applied first for n_2 cycles, the damage is

$$D_{n_2} = 1 - (1 - D_0) \prod_{i=1}^{n_2} f(\underline{\epsilon}_{2_i};\Omega) \tag{35}$$

This is followed by S_1 for n_1 cycles. The total damage is

$$D_{n_2,n_1} = 1 - (1 - D_{n_2}) \prod_{i=n_2+1}^{n_1+n_2} f(\underline{\epsilon}_{1_i};\Omega) \tag{36}$$

$$= 1 - (1 - D_0) \prod_{i=1}^{n_2} f(\underline{\epsilon}_{2_i};\Omega) \prod_{i=n_2+1}^{n_1+n_2} f(\underline{\epsilon}_{1_i};\Omega) \tag{37}$$

It is obvious that D_{n_1,n_2} in general is different from D_{n_2,n_1}. We can, however, find a condition that would make these two equal, and the Miner linear cumulative fatigue damage rule valid. Consider,

$$\underline{\epsilon}_{1_i} = \underline{\epsilon}_1, \forall i \in [1, n_1 + n_2] \tag{38}$$

$$\underline{\epsilon}_{2_i} = \underline{\epsilon}_2, \forall i \in [1, n_1 + n_2] \tag{39}$$

which means the strain limits in every cycle are independent of the past. Under this condition,

$$D_{n_1,n_2} = 1 - (1 - D_0) \prod_{i=1}^{n_1} f(\underline{\epsilon}_1;\Omega) \prod_{i=n_1+1}^{n_1+n_2} f(\underline{\epsilon}_2;\Omega) \tag{40}$$

$$= 1 - (1 - D_0) f^{n_1}(\underline{\epsilon}_1;\Omega) f^{n_2}(\underline{\epsilon}_2;\Omega) \tag{41}$$

and

$$D_{n_2,n_1} = 1 - (1 - D_0) \prod_{i=1}^{n_2} f(\underline{\epsilon}_2;\Omega) \prod_{i=n_2+1}^{n_1+n_2} f(\underline{\epsilon}_1;\Omega) \tag{42}$$

$$= 1 - (1 - D_0) f^{n_2}(\underline{\epsilon}_2;\Omega) f^{n_1}(\underline{\epsilon}_1;\Omega) \tag{43}$$

Under these conditions, the two accumulated damages are equal. In other words, if no strain hardening or softening occurs during fatigue cycling, and if the cycling takes place between exactly the same strain limits for a given load level (irrespective of where in the life of the component this load is applied), then the load sequencing effect vanishes and Miner's rule is valid. Of course, these conditions may often be unrealistic in practice.

Figure 7 shows two different (predicted) fatigue damage growth trajectories in SAE 4340 steel under stress-controlled cycling: one due to a high–low sequence and the other due to a low–high sequence, with $S_1 = \pm 690$ MPa (± 100 ksi), $n_1 = 100$ and $S_2 = \pm 827$ MPa (± 120 ksi), $n_2 = 20$. The damage caused by the high–low sequence after $n_1 + n_2 = 120$ cycles is $D_{n_2,n_1} = 0.9$ (Equation (37)), whereas the damage caused by the low–high sequence after the same number of cycles is much less ($D_{n_1,n_2} = 0.25$ from Equation (34)). This agrees with observed trends in fatigue load-sequencing[14].

Figure 8 shows the various combinations of cycle ratios n_1/N_1 and n_2/N_2 that lead to (predicted) crack

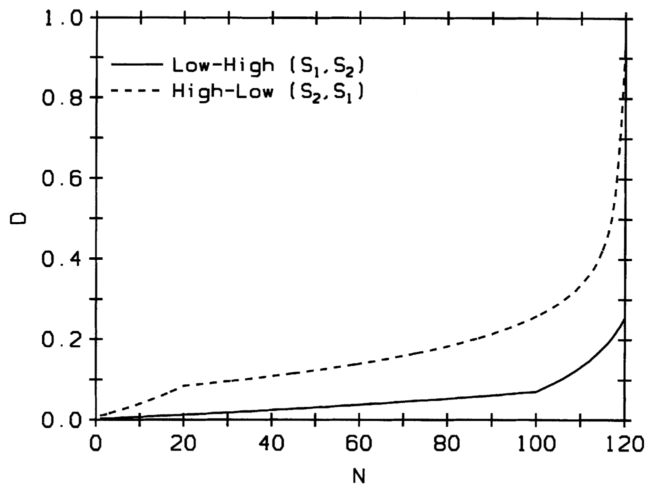

Figure 7 Effect of load sequencing on damage growth in stress-controlled fatigue of SAE 4340 steel, $S_2 > S_1$

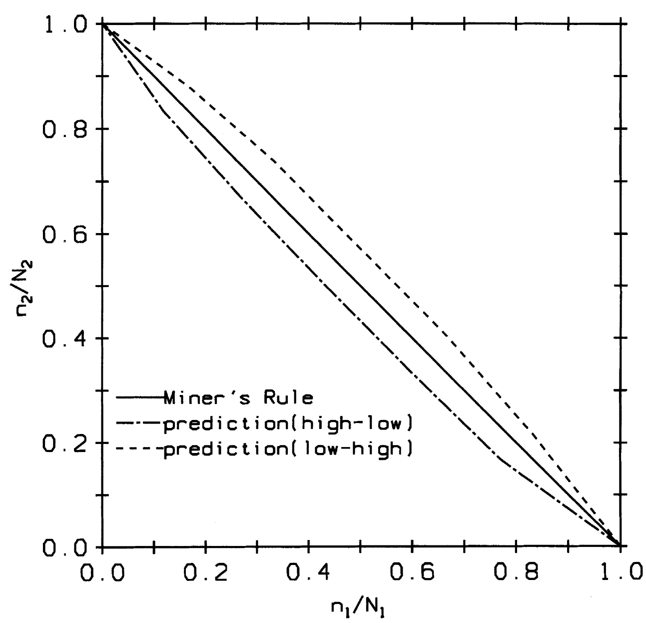

Figure 8 Predicted failure (i.e. crack initiation) in two-level stress-controlled fatigue cycling of SAE 4340 steel

initiation after $n_1 + n_2$ cycles of two-level stress-controlled cycling of SAE 4340 steel. As before, $S_1 = \pm\ 690$ MPa and $S_2 = \pm\ 827$ MPa; the predicted cycles to crack initiation are $N_1 = 210$ and $N_2 = 42$, respectively, corresponding to $D_c = 0.46$. The initiation life under two-level cycling is lower if the higher stress is applied first, which is evident in *Figure 8*. As an example, if 14 cycles of S_2 are applied first, only 124 cycles of S_1 may be applied before crack initiation occurs. However, the same 14 cycles of S_2 may be preceded by 153 cycles of S_1 if S_1 is applied first, resulting in a 21% increase in N_I. Miner's rule, however, plots as a straight line and cannot distinguish between the ordering of the blocks; it predicts $N_I = 154$ regardless of where the large cycles occur.

Figure 9 shows the effect of high to low stress-controlled cycling on fatigue crack initiation and failure of SAE 4130 steel. Fatigue damage growth is computed with the help of Equation (37) using material properties from *Table 1*, and the initiation life is determined from

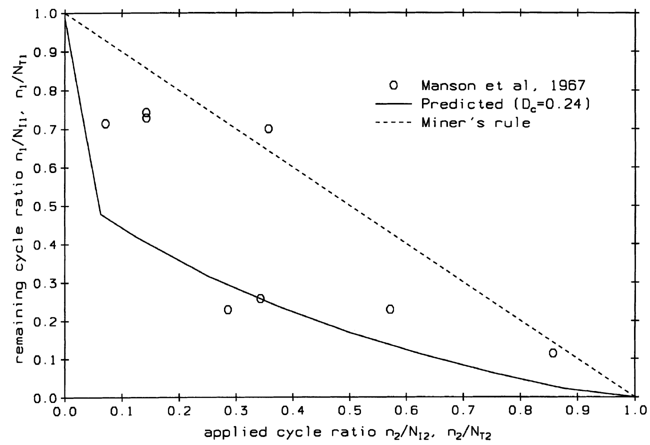

Figure 9 Effect of high to low load sequencing on crack initiation and fatigue life of SAE 4130 steel

Equation (17) with $D_c = 0.24$, obtained from a monotonic ductile damage growth experiment on French 30CD4 (equivalent to SAE 4130) reported by Lemaitre (1985)[45]. The predicted relation between applied and remaining cycle ratios to crack initiation plots to the left of the Miner line, and agrees qualitatively with the corresponding experimental fatigue data.

CONCLUSION

Starting with the first principles of thermodynamics and mechanics, a CDM-based model for predicting fatigue crack initiation was developed in this paper. The proposed model uses only readily available macroscopic material properties. Fatigue damage is computed recursively as a function of elapsed cycles, which facilitates the inclusion of variable amplitude loading from cycle to cycle. The effects of strain-controlled and stress-controlled load cyclings can be differentiated, mean stress effects can be exhibited, and load sequencing effects were predicted correctly. Although the loading was treated deterministically in this analysis, random loading can be incorporated without much difficulty by treating σ_∞ in Equation (15) as a random process.

The CDM analysis presented herein in based on the notion of isotropic damage that is volumetrically homogeneous prior to localization. There is evidence that fatigue damage prior to initiation is a surface-related rather than a volume-related phenomenon. The prediction of crack initiation behavior herein agreed reasonably well with experimental data. Additional research aimed at incorporating any surface-related effect within the CDM framework may lead to further improvements.

ACKNOWLEDGEMENT

Support for this research, provided, in part, by Lockheed–Martin Energy Research Corporation under award 19X-SP638V, with Dr D. J. Naus as Program Manager, is gratefully acknowledged. The authors would also like to thank Mr Omesh Chopra of Argonne National Laboratory for making available the fatigue loading data used in this paper.

REFERENCES

1 Murtaza, G. and Akid, R., Modelling short fatigue crack growth in a heat-treated low-alloy steel. *International Journal of Fatigue*, 1995, **17**(3), 207–214.

2 Dowling, N., *Mechanical Behavior of Materials*. Prentice Hall, Englewood Cliffs, NJ, 1993.

3 Klesnil, M., Polak, J. and Liskutin, P., Short crack growth close to the fatigue limit in low carbon steel. *Scripta Metallurgica*, 1984, **18**(11), 1231–1234.

4 Kaynak, C. and Ankara, A., Short fatigue crack growth in Al 2024-T3 and Al 7075-T6. *Engineering Fracture Mechanics*, 1992, **43**(5), 769–778.

5 Kaynak, C., Ankara, A. and Baker, T. J., Effects of short cracks on fatigue life calculations. *International Journal of Fatigue*, 1996, **18**(1), 25–31.

6 Martin, W. S. and Wirsching, P. H., Fatigue crack initiation–propagation reliability model. *Journal of Materials in Civil Engineering, ASCE*, 1991, **3**(1), 1–18.

7 Min, L., Qing, S. and Qing-Xiong, Y., Large sample size experimental investigation on the statistical nature of fatigue crack initiation and growth. *International Journal of Fatigue*, 1996, **18**(2), 87–94.

8 Kujawski, D. and Ellyin, F., Crack initiation and total fatigue life of a carbon steel in vacuum and air. *Journal of Testing and Evaluation*, 1992, **20**(6), 391–395.

9 Majumdar, S., Chopra, O. K. and Shack, W. J., Interim failure design curves for carbon, low-alloy, and austenitic stainless steels in LWR environments. In *Proceedings of 20th WRSM*, Vol. 3, NUREG/CP-0126, 3 March 1993.

10 Committee on Fatigue and Fracture Reliability (1982) Fatigue reliability, Journal of the Structural Division, ASCE, 108(ST1), 1–88.

11 Grover, H. J., *Fatigue of Metals and Structures*. US Government Printing Office, Washington, 1954.

12 Schutz, W., Fatigue life prediction—a review of the state of the art. In *Structural Failure, Product Liability and Technical Insurance*, Vol. IV, ed. T. Rossmanith, Elsevier, 1993.

13 Miner, M. A., Cumulative damage in fatigue. *Journal of Applied Mechanics*, 1945, **12**, A159–A164.

14 Kutt, T. V. and Bieniek, M. P., Cumulative damage and fatigue life prediction. *AIAA Journal*, 1988, **26**(2), 213–219.

15 Wheeler, O. E., Spectrum loading and crack growth. *Journal of Basic Engineering*, 1972, **94**, 181–186.

16 Paas, M. H. J. W., Schreurs, P. J. G. and Brekelmans, W. A. M., A continuum approach to brittle and fatigue damage: theory and numerical procedures. *International Journal of Solids and Structures*, 1993, **30**(4), 579–599.

17 Pasic, H., A unified approach of fracture and damage mechanics to fatigue damage problems. *International Journal of Solids and Structures*, 1992, **29**(14/15), 1957–1968.

18 Tiejun, W. and Zhiwen, L., A continuum damage model for weld heat affected zone under low cycle fatigue loading. *Engineering Fracture Mechanics*, 1990, **37**(4), 825–829.

19 Manson, S. S., Freche, J. C. and Ensign, C. R., Application of a double linear damage rule to cumulative fatigue. *Fatigue Crack Propagation, ASTM STP*, 1967, **415**, 384–412.

20 Miller, K. J. and Zachariah, K. P., Cumulative damage laws for fatigue crack initiation and stage I propagation. *Journal of Strain Analysis*, 1977, **12**(4), 262–270.

21 Hashin, Z. and Rotem, A., A cumulative damage theory of fatigue failure. *Materials Science and Engineering*, 1978, **34**, 147–160.

22 Krajcinovic, D., Continuum damage mechanics. *Applied Mechanics Reviews*, 1984, **37**(1), 1–6.

23 Simo, J. C. and Ju, J. W., Strain and stress-based continuum damage models–I. *International Journal of Solids and Structures*, 1987, **23**(7), 821–840.

24 Hult, J., Introduction and general overview. In *Continuum Damage Mechanics Theory and Applications*, eds. D. Krajcinovic and J. Lemaitre, Springer–Verlag, New York, 1987.

25 Hansen, N. R. and Schreyer, H. L., A thermodynamically consistent framework for theories of elastoplasticity coupled with damage. *International Journal of Solids and Structures*, 1994, **31**(3), 359–389.

26 Chaboche, J. L., Continuum damage mechanics–I and II. *Journal of Applied Mechanics*, 1988, **55**, 59–72.

27 Lemaitre, J., How to use damage mechanics. *Nuclear Engineering and Design*, 1984, **80**, 233–245.

28 Dhar, S., Sethuraman, R. and Dixit, P. M., A continuum damage mechanics model for void growth and micro crack initiation. *Engineering Fracture Mechanics*, 1996, **53**(6), 917–928.

29 Chow, C. L. and Wei, Y., A damage mechanics model of fatigue crack initiation in notched plates. *Theoretical and Applied Fracture Mechanics*, 1991, **16**, 123–133.

30 Lemaitre, J., *A Course on Damage Mechanics*. Springer–Verlag, Dordrecht, The Netherlands, 1992.

31 Kachanov, L. M., *Introduction to Continuum Damage Mechanics*. Martinus Nijhoff, 1986.

32 DeVree, J. H. P., Brekelmans, W. A. M. and Van Gils, M. A.J., Comparison of nonlocal approaches in continuum damage mechanics. *Computers and Structures*, 1995, **55**(4), 581–588.

33 Sears, F. W. and Salinger, G. L., *Thermodynamics, Kinetic Theory and Statistical Thermodynamics*. Addison–Wesley, Reading, MA, 1975.

34 McLellan, A. G., *The Classical Thermodynamics of Deformable Materials*. Cambridge University Press, Cambridge, UK, 1980.

35 Bhattacharya, B., A damage mechanics-based approach to structural deterioration and reliability. PhD Thesis, The Johns Hopkins University, Baltimore, MD 21218, USA, 1997.

36 Maugin, G. A., *The Thermomechanics of Plasticity and Fracture*. Cambridge University Press, Cambridge, UK, 1992.

37 Krajcinovic, D. and Sumarac, D., Micromechanics of the damage process. In *Continuum Damage Mechanics Theory and Applications*, ed. D. Krajcinovic and J. Lemaitre. Springer–Verlag, New York, 1987.

38 Endo, T. and Morrow, J., Cyclic stress–strain and fatigue behavior of representative aircraft metals. *Journal of Materials JMLSA*, 1969, **4**(1), 159–175.

39 Chopra, O. K. et al., Environmentally assisted cracking in light water reactors. Report NUREG/CR-4667 ANL-95/2 Vol. 19. US Nuclear Regulatory Commission, Washington, DC, 1995.

40 Boller, C. and Seeger, T., *Materials Data for Cyclic Loading, part B*. Elsevier, Amsterdam, The Netherlands, 1987.

41 Topper, T. H. and Morrow, J., Simulation of the fatigue behavior at the notch root in spectrum loaded notched members. T. and A. M. Report no 333, Department of Theoretical and Applied Mechanics, University of Illinois, Urbana, IL, 1970.

42 Barsom, J. M. and Rolfe, S. T., *Fracture and Fatigue Control in Structures*, Prentice–Hall, Englewood Cliffs, NJ, 1987.

43 Chopra, O. K., (of Argonne National Laboratory, Argonne, IL 60439, USA) Personal communication to B. R. Ellingwood regarding report NUREG/CR-6237, 1996.

44 Boyer, H. E., *Atlas of Stress–Strain Curves*. ASM International, Metals Park, OH, 1987.

45 Lemaitre, J., A continuous damage mechanics model for ductile fracture. *Journal of Engineering Materials and Technology*, 1985, **107**(1), 83–89.